ISSN 1063-7834, Physics of the Solid State, 2012, Vol. 54, No. 7, pp. 1408–1416. © Pleiades Publishing, Ltd., 2012.
Original Russian Text © E.A. Podolskaya, A.M. Krivtsov, 2012, published in Fizika Tverdogo Tela, 2012, Vol. 54, No. 7, pp. 1327–1334.

MECHANICAL PROPERTIES, PHYSICS OF STRENGTH, AND PLASTICITY

Description of the Geometry of Crystals with a Hexagonal Close-Packed Structure Based on Pair Interaction Potentials

E. A. Podolskaya* and A. M. Krivtsov

Institute of Problems in Mechanical Engineering, Russian Academy of Sciences, Bolshoj pr. 61, St. Petersburg, 199178 Russia

** e-mail: katepodolskaya@gmail.com*

Received July 11, 2011; in final form, October 12, 2011

Abstract—The pair force interaction potential that allows one to describe a deviation from spherical symmetry, which is typical for hexagonal close-packed structures, is constructed using the "spherically symmetric" Mie potential that depends only on the interatomic distance. The parameters of the considered potential, which ensure the stability of hexagonal close-packed lattices, are obtained for a wide range of metals, namely, beryllium, gadolinium, hafnium, holmium, dysprosium, yttrium, cobalt, lutetium, magnesium, osmium, rhenium, ruthenium, scandium, thallium, terbium, technetium, titanium, thulium, cerium, zirconium, and erbium. It is shown that for this pair interaction potential the hexagonal close-packed structure is energetically more favorable than the face-centered cubic structure. The proposed potential can be used to perform computational experiments and analytical investigations.

DOI: 10.1134/S1063783412070311

1. INTRODUCTION

In recent years, there have appeared a large number of publications by Russian and foreign scientists, devoted to computer simulation [1–5] and analytical investigation [1, 5–9] of solids with microstructure. The interest in these objects is associated, to a large extent, with the development of nanotechnologies. For example, carbon nanotubes are considered in [3, 7]. Small sizes and discrete structure of these materials lead to the necessity of using atomistic approaches. It is usually assumed that a medium with microstructure can be represented by an ensemble of material points or solids that model, for example, crystal lattice nodes and interact with each other via a potential the parameters of which are determined from a comparison between physical properties of the model and real materials. For this purpose, it is necessary to find a relationship between the characteristics obtained within the discrete approach and the continuum parameters [2, 5–7].

A common model of media with microstructure is the crystal lattice. The "spherically symmetric" pair force interaction potentials, which depend only on the distance between the atoms, are effectively used for both analytical description and numerical simulation of close-packed lattices. In the case of non-close-packed structures, this approach can lead to the problems associated with the instability of the model material. Therefore, it is common practice to consider either many-body interaction [10] or moment interaction [11].

A frequently encountered crystal structure is the hexagonal close-packed (HCP) structure, which is typical for many metals. According to [12], the bond in a metal crystal is non-directional, i.e., "spherically symmetric"; consequently, in crystallography, a real metal atom is replaced by a hard sphere with the radius—the so-called metallic radius of atom—equal to half of the distance between the nearest neighbor atoms. A perfect close-packed lattice consists of hard spheres packed in layers within a particular volume. The lattice of real HCP metals has a lower density of packing, which corresponds to the packing of the ellipsoids of revolution rather than spheres. In the majority of cases, the ratio of the semiaxes of the ellipsoid differs from 1 by no more than 4%.

The description of metals is usually performed using the embedded atom potential [13], which correctly describes some of the HCP metals [14]. The adequate description of other HCP metals requires a modification [15] associated with the introduction of additional terms that take into account the change in the angle between the bonds. The modified embedded atom potentials, which ensure the stability of the HCP lattice for a number of metals, were constructed in [16, 17]. The embedded atom potential has a large number of parameters that allows one to describe the elastic and energy characteristics. However, as well as in the case of the moment interaction, the procedures used for fitting of the parameters and numerical simulation are much more complicated in comparison with the pair force interaction. In [18], it was proposed to use the so-called anisotropic interatomic interaction potential, which depends on the angle between the

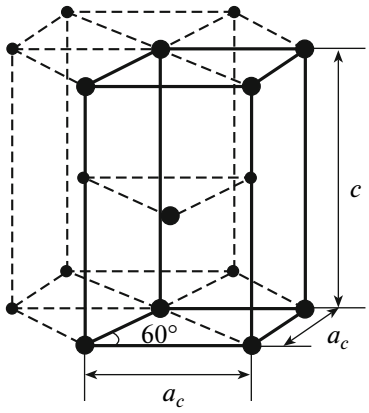

Fig. 1. Unit cell of HCP lattice.

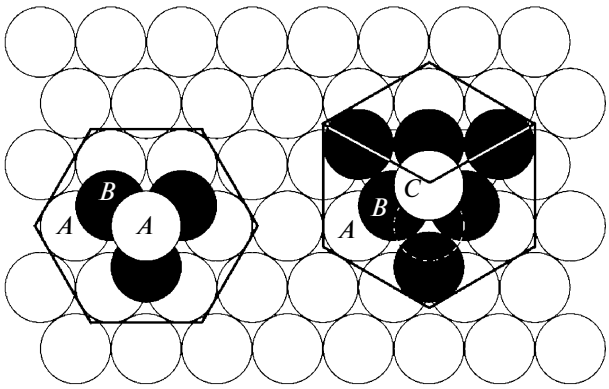

Fig. 2. Visualization of HCP (left) and FCC (right) structures.

bonds. The symmetry of the crystal lattice in this case is reflected by the potential function.

In [19], it was shown that the elastic properties of HCP metals from the B-subgroup of the Periodic Table (transition elements) are fairly well described using the pair force interaction models. In the present paper, we consider the possibility of adequate description of HCP structures with the use of a pair force interaction potential which contains a small number of parameters, does not depend on the structure of the lattice of real HCP metals, and ensures their stable equilibrium. Under the conditions of the formulated problem, we use spline potentials in order to exclude atoms outside the so-called cut-off radius from consideration [2, 20, 21]. For the chosen potential, we verify the stability and energetic favorability of the model.

2. HEXAGONAL CLOSE-PACKED STRUCTURE

The unit cell of an HCP lattice consists of parallel rhombi with the side a_c and the angle of 60°, which are spaced at the distance c. An additional atom is located on the middle plane between the bases of the cell. The triple unit cell, which is frequently depicted (Fig. 1), has a regular hexagon, which is formed by three rhombi, in the base. The lattice of real HCP metals is characterized by the parameter

$$\eta = c/a_c.$$

For the parameter $\eta = \eta_0 = 2\sqrt{2/3}$, we have the closest packing of the atoms. Let us also introduce the dimensionless parameter $\zeta = (\eta - \eta_0)/\eta_0$.

Figure 2 shows two most frequently encountered close-packed structures, i.e., HCP and face-centered cubic (FCC) structures, as a sequence of spherical layers of two and three types, respectively. HCP structure has a two-layer periodicity, and the sequence of layers of this structure is written as ...*ABABAB*.... FCC structure has a three-layer periodicity, which is characterized by the sequence ...*ABCABCABC*.... Both structures have an identical packing density, which is equal to the ratio of the total volume occupied by the actual atoms in the crystal lattice to the total volume of the crystal lattice itself; however, these crystal structures have significant topological differences. FCC lattice is simple: all the atoms (*A*, *B*, and *C*) are located in identical positions with respect to their environment. HCP lattice is complex diatomic: with respect to the atoms in the even (*B*) and odd (*A*) layers, their surroundings are arranged differently. Let us consider that the atoms located in the even and odd layers are of different types, even though the atoms themselves are identical and only the geometry of their surrounding differs. Any complex lattice can be represented as several simple sublattices inserted into each other. For HCP lattice, there are two simple sublattices, and they can be obtained as a combination of the even and odd layers of atoms, respectively. For a perfect HCP structure, the double relative distance between the layers is $\eta_0 = 2\sqrt{2/3}$, while in the lattice of real HCP metals, this distance can significantly differ from η_0. For metals with FCC lattice, these differences are not observed. Thus, the lattice of metals that crystallize in HCP structure will be described not by the close packing of hard spheres but by the close packing of the ellipsoids of revolution that are elongated or flattened in comparison with the sphere along the axis perpendicular to the layer plane. Figure 3 shows metals with HCP structure. In this figure, the dark-gray areas indicate metals for which the double distance between the layers is less than the parameter η_0 (Be, Mg, Sc, Ti, Co, Y, Zr, Tc, Ru, Hf, Re, Os, Tl, Gd, Tb, Dy, Ho, Er, Tm, Lu), and the light-gray areas indicate metals for which this distance is larger than η_0 (Zn, Cd, La, Ce, Pr, Nd, Pm, Am, Cm, Bk, Cf) [22].

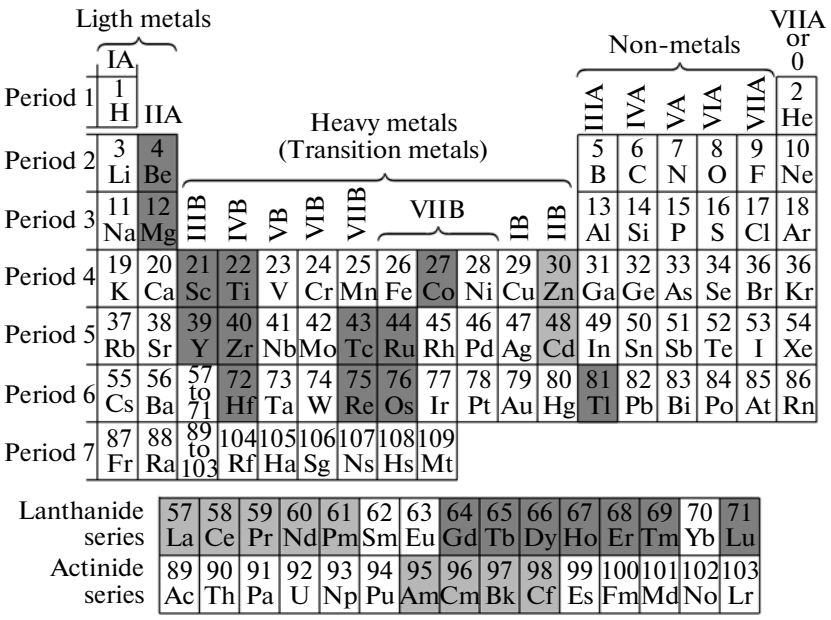

Fig. 3. Metals with HCP structure.

3. CONSTRUCTION OF THE INTERACTION POTENTIAL

We introduce the coordination tensor defined by the expression [8]

$$\mathbf{A} = \sum_{\alpha} \mathbf{n}_{\alpha}\mathbf{n}_{\alpha}. \qquad (1)$$

Here, $\mathbf{n}_{\alpha}$ are the unit vectors of the directions of the bonds passing from the reference atom to the atom with the number α. The summation is performed over all the atoms that interact with the reference atom. The type of reference atom does not matter.

Let us consider the equilibrium of 12 nearest neighbors of the reference atom without regard for the influence exerted by the next atoms. For a perfect HCP structure, the coordination tensor for the 12 nearest neighbors of the reference atom is spherical. Hence, we can say that these atoms form the first coordination sphere. For real metals, the asymmetry of the structure leads to the asymmetry of the coordination tensor, making it transversely isotropic. The plane of isotropy of the tensor coincides with the plane of the layers. Therefore, the 12 nearest neighbors of the reference atom should be referred to as the first coordination ellipsoid.

Now, we turn to Fig. 4. Here, we use the following notation: 0 is the reference atom; 1, 2, and 3 are the atoms located on the first, second, and third coordination ellipsoids, respectively; and $3a$ are the atoms which lie between the second and third coordination ellipsoids if the parameter $\zeta < 1.33\%$ (all metals marked by dark-gray color in Fig. 3 and cerium), or which lie between the third and fourth coordination ellipsoids if $\zeta > 13\%$ (all metals marked by light-gray color in Fig. 3, except for cerium). Metals characterized by the parameter ζ in the range $1.33\% < \zeta < 13.0\%$ do not exist. It should be noted that the tables [18, 23] provide the values of R_0, R, and η, where R_0 is the distance between the reference atom and its nearest neighbors located in the same layer as this reference atom, R is the distance between the reference atom and its nearest neighbors located in the adjacent layers, and $\eta = 2\sqrt{R^2/R_0^2 - 1/3}$ is the double distance between the layers. The distances between the reference atom and the atoms located on the first coordination ellipsoid are equal to R_0 and R; the distances between the reference atom and the atoms located on the second coordination ellipsoid are equal to $\sqrt{R_0^2 + R^2}$; the distances between the reference atom and the atoms located on the third coordination ellipsoid are equal to $R_0\sqrt{3}$ and $\sqrt{2R_0^2 + R^2}$; and the distances between the reference atom and the atoms $3a$ are equal to ηR_0.

According to [2], the stress tensor in a simple lattice with pair force interatomic interaction has the form

$$\boldsymbol{\tau} = -\frac{1}{2V_0}\sum_{\alpha} a_{\alpha} f(a_{\alpha}) \mathbf{n}_{\alpha}\mathbf{n}_{\alpha}, \qquad (2)$$

where $f(r) = -\Pi'(r)$ is the interaction force, $\Pi(r)$ is the interaction potential, and V_0 is the unit cell volume; for HCP lattice, the unit cell represents a right prism with the base in the form of a rhombus with the angle of 60° (see Fig. 1). For a complex lattice, the stress tensor has the form $\boldsymbol{\tau} = \sum_\gamma \boldsymbol{\tau}_\gamma$, where $\boldsymbol{\tau}_\gamma$ is calculated by formula (2). In the case of diatomic HCP lattice, $\gamma = 2$. It can be shown that $\boldsymbol{\tau}_1 \equiv \boldsymbol{\tau}_2$. Therefore, the equilibrium condition for HCP structure in the absence of external forces takes the form

$$\boldsymbol{\tau} = 0. \tag{3}$$

If we considered a perfect HCP structure, the stress tensor would be spherical, and, instead of a single tensor equation, which is equivalent to six scalar equations (because $\boldsymbol{\tau} = \boldsymbol{\tau}^T$), we would obtain a single scalar equation. Due to specific features of HCP lattice, the stress tensor $\boldsymbol{\tau}$ contains two components:

$$\boldsymbol{\tau} = \hat{\tau}\mathbf{E} + (\tau_e - \hat{\tau})\mathbf{ee}, \tag{4}$$

where $\mathbf{e}$ is the unit vector of the axis perpendicular to the layer plane, i.e., the unit vector of the symmetry axis of the coordination tensor. In the equilibrium position, the stress tensor components $\hat{\tau}$ and τ_e should vanish.

It is obvious that, for a perfect lattice, we have the equality $\hat{\tau} = \tau_e$. If we take only the first coordination ellipsoid into consideration and ignore the interaction with the next atoms, the tensor components $\hat{\tau}$ and τ_e are determined from the stress tensor (2) by

$$\begin{aligned} -2V_0\hat{\tau} &= 3R_0 f(R_0) + \frac{12}{4+3\eta^2} Rf(R), \\ -2V_0\tau_e &= \frac{18}{4+3\eta^2} Rf(R). \end{aligned} \tag{5}$$

We assume that the pair interaction potential allows only one equilibrium position $f(a) = 0$. Then, from the second equation (5), it follows that

$$f(R) \equiv 0 \Leftrightarrow R = a. \tag{6}$$

From the first equation of (5) and (6), we obtain

$$f(R_0) \equiv 0 \Leftrightarrow R = R_0 = a \Leftrightarrow \eta = \eta_0. \tag{7}$$

Therefore, considering the first coordination ellipsoid, we cannot describe the geometric imperfection of HCP lattice with the use of a "spherically symmetric" interaction force.

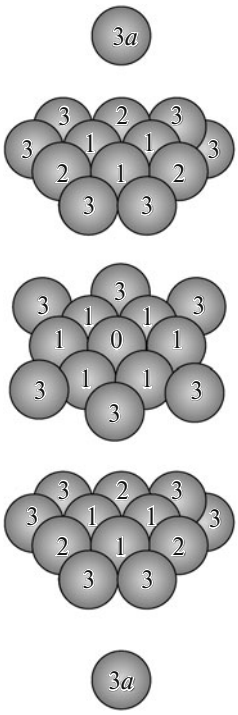

Fig. 4. Considered coordination ellipsoids.

Taking into account the second coordination ellipsoid and using (2), we obtain

$$\begin{aligned} -2V_0\hat{\tau} &= 3R_0 f(R_0) + \frac{12R}{4+3\eta^2} f(R) \\ &+ \frac{48\sqrt{R_0^2+R^2}}{16+3\eta^2} f(\sqrt{R_0^2+R^2}), \\ -2V_0\tau_e &= \frac{18}{4+3\eta^2} Rf(R) \\ &+ \frac{18\eta^2\sqrt{R_0^2+R^2}}{16+3\eta^2} f(\sqrt{R_0^2+R^2}). \end{aligned} \tag{8}$$

It can be shown that, in this case, the solution of the problem for the interaction through the "spherically symmetric" potential also leads to the identical equality $R = R_0$ too. This can be verified by setting arbitrary values of the potential parameters and solving equations (8) for the variables R_0 and R. The obtained result is most likely a consequence of the fact that the coordination tensor composed of atoms of the second coordination ellipsoid is spherical. Therefore, in order to describe the geometric imperfection of the HCP structure, it is necessary to consider a greater number of coordination ellipsoids.

Taking into account atoms 3 and 3*a* (Fig. 4), the components of the stress tensor are determined by

$$-2V_0\hat{\tau} = 3R_0 f(R_0) + \frac{12R}{4+3\eta^2} f(R)$$
$$+ \frac{48\sqrt{R_0^2+R^2}}{16+3\eta^2} f(\sqrt{R_0^2+R^2}) + 3\sqrt{3}R_0 f(\sqrt{3}R_0)$$
$$+ \frac{168\sqrt{2R_0^2+R^2}}{28+3\eta^2} f(\sqrt{R_0^{22}+R^2}), \quad (9)$$

$$-2V_0\tau_e = \frac{18}{4+3\eta^2} Rf(R) + \frac{18\eta^2\sqrt{R_0^2+R^2}}{16+3\eta^2} f(\sqrt{R_0^2+R^2})$$
$$+ \frac{36\eta^2\sqrt{2R_0^2+R^2}}{28+3\eta^2} f(\sqrt{2R_0^2+R^2}) + 2\eta R_0 f(\eta R_0).$$

The next step is to choose a particular pair interaction potential so that, on the one hand, it would satisfy the equilibrium equations and, on the other hand, it would allow for a unique equilibrium position and provide the repulsion and attraction of the particles with a decrease and an increase in the interparticle distance, respectively. Moreover, it is necessary to substantiate the possibility of disregarding the forces of interaction with more distant atoms. For these purposes, it is convenient to use the spline potential, which is commonly used to accelerate numerical calculations. We introduce the cut-off radius a_{cut} so that $f(r) \equiv 0$ for $r > a_{cut}$. The spline potential can be constructed from a pair force interaction potential in different ways [2, 20, 21]. Since the stress tensor includes the interaction forces, we choose the type of potential which has the simplest expression for the forces [2]

$$\tilde{f}(r) = k(r)f(r), \quad (10)$$

where $k(r)$ is the smoothing function:

$$k(r) = \begin{cases} 1, & r \le b, \\ \left(1 - \left(\dfrac{r^2-b^2}{a_{cut}^2-b^2}\right)^2\right)^2, & b < r \le a_{cut}, \\ 0, & r > a_{cut}. \end{cases} \quad (11)$$

Here, b is the critical distance at which the interatomic bond is broken (it is determined from the condition $f'(b) = 0$). In addition, for this potential, the cut-off radius a_{cut} is chosen arbitrarily, and the potential is continuous up to and including the second derivative. This potential is calculated by

$$\tilde{\Pi}(r) = \int_r^{a_{cut}} k'(r)\Pi(r)dr + k(r)\Pi(r) - k(a_{cut})\Pi(a_{cut}). \quad (12)$$

The base potential $\Pi(r)$, for which the corresponding force is multiplied by the smoothing function (see expression (10)), is taken as the Mie potential

$$\Pi(r) = \frac{D}{n-m}\left(m\left(\frac{a}{r}\right)^n - n\left(\frac{a}{r}\right)^m\right). \quad (13)$$

Here, D is the depth of the potential well and a is the equilibrium distance. Then, the critical distance is determined by the relationship $b = a^{(n-m)}\sqrt{(n+1)/(m+1)}$. So, in the spline potential, we have four parameters: a, a_{cut}, n, and m. The depth of the potential well D is temporarily excluded from consideration, because, upon the substitution of the interaction force into the equilibrium equations (9), it is factored out from the parentheses.

We propose the following method for determining the parameters a, a_{cut}, n, and m. Let us transform equations (9) into the dimensionless form and set the right-hand sides equal to zero:

$$\bar{f} = \frac{fa(n-m)}{Dnm},$$
$$f_{10} = \bar{f}(R_0), \quad f_1 = \bar{f}(R), \quad f_2 = \bar{f}(\sqrt{R_0^2+R^2}), \quad (14)$$
$$f_{30} = \bar{f}(\sqrt{3}R_0), \quad f_3 = \bar{f}(\sqrt{2R_0^2+R^2}), \quad f_4 = \bar{f}(\eta R_0).$$

$$\bar{F} = 2f_{10} + 2\sqrt{\frac{3}{4+3\eta^2}} f_1 + 8\sqrt{\frac{3}{16+3\eta^2}} f_2 + 3\sqrt{3}f_{30} + 28\sqrt{\frac{3}{28+3\eta^2}} f_3 = 0,$$
$$\bar{F}_e = 3\sqrt{\frac{3}{4+3\eta^2}} f_1 + 3\eta^2\sqrt{\frac{3}{16+3\eta^2}} f_2 + 6\eta^2\sqrt{\frac{3}{28+3\eta^2}} f_3 + 2\eta f_4 = 0. \quad (15)$$

Next, we introduce $\rho = R_0/a$ and $\rho_{cut} = a_{cut}/a$ so that the dimensionless interaction forces depend on the dimensionless parameters.

In order to determine the parameters ρ, ρ_{cut}, n, and m, we minimize the sum of the squares of the left-hand sides of equations (15) according to the following scheme:

(i) The parameters n and m are varied from 1 to 10 under the condition $n > m$ so that the resulting poten-

tial provides the repulsion and attraction of the particles with a decrease and an increase in the interparticle distance, respectively.

(ii) The equilibrium distance of the potential should be larger than the radius of the first coordination sphere; however, in this case, it should be taken into account that the addition of only three coordination spheres cannot lead to a significant change in the distance between the nearest neighbor atoms [2]

$$0.8 \le \rho \le 1.0. \quad (16)$$

(iii) The cut-off radius should be such that all the considered atoms would be inside the region bounded by it and the next atoms would be outside this region.

(a) For $\zeta \le 0\%$ (all metals marked by dark-gray color in Fig. 3), we have

$$\sqrt{3}\rho \le \rho_{cut} \le \sqrt{1+\eta^2}\rho. \quad (17)$$

(b) For $\zeta = 1.33\%$ (cerium), we have

$$\rho\sqrt{(28+3\eta^2)/12} \le \rho_{cut} \le \sqrt{1+\eta^2}\rho. \quad (18)$$

(c) For $\zeta \ge 13\%$ (all metals marked by light-gray color in Fig. 3, except for cerium), we have

$$\eta\rho \le \rho_{cut} \le 2\rho. \quad (19)$$

4. VERIFICATION OF THE STABILITY

After the potential providing the equilibrium of the real HCP structure is constructed, it is necessary to find out whether this equilibrium position is stable. For this purpose, according to [24, 25, 28], we should analyze the stiffness tensor for the positive definiteness. The stiffness tensor of a complex diatomic lattice has the form [2, 8]

$$^4\mathbf{C} = {}^4\mathbf{C}_* - {}^3\mathbf{C}\cdot{}^2\mathbf{C}^{-1}\cdot{}^3\mathbf{C}, \quad (20)$$

$$^2\mathbf{C} = \frac{1}{V_0}\sum_\alpha \frac{v_\alpha}{a_\alpha}[(a_\alpha\Pi''(a_\alpha) - \Pi'(a_\alpha))\mathbf{n}_\alpha\mathbf{n}_\alpha + \Pi'(a_\alpha)\mathbf{E}],$$

$$^3\mathbf{C} = \frac{1}{V_0}\sum_\alpha v_\alpha(a_\alpha\Pi''(a_\alpha) - \Pi'(a_\alpha))\mathbf{n}_\alpha\mathbf{n}_\alpha\mathbf{n}_\alpha, \quad (21)$$

$$^4\mathbf{C}_* = \frac{1}{V_0}\sum_\alpha a_\alpha(a_\alpha\Pi''(a_\alpha) - \Pi'(a_\alpha))\mathbf{n}_\alpha\mathbf{n}_\alpha\mathbf{n}_\alpha\mathbf{n}_\alpha,$$

where $\mathbf{n}_\alpha$ are the unit vectors of the directions of the bonds, a_α are the bond lengths, $v_\alpha = 0$ if atoms of the same type interact with each other, $v_\alpha = 1$ if atoms of different types interact with each other, $\mathbf{E}$ is the identity tensor, $\Pi(a_\alpha)$ is the interaction potential of the reference atom with the atom under the number α, and V_0 is the unit cell volume. The summation is performed over all the atoms that interact with the reference atom. The type of reference atom does not matter.

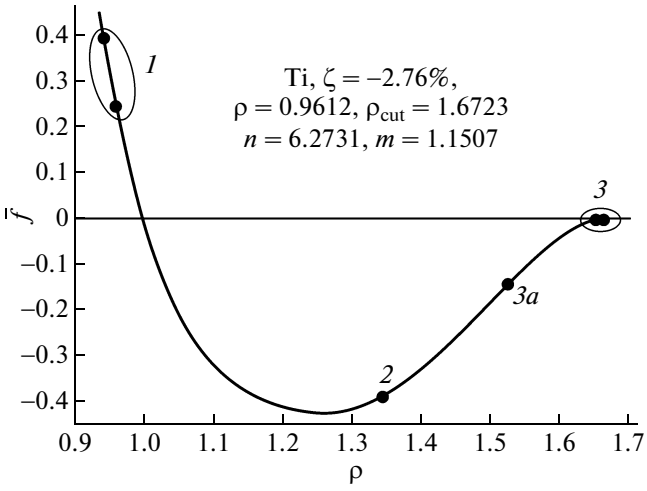

Fig. 5. An example of the interaction force (titanium).

The deformation of a complex lattice involves the deformation of the sublattices and their displacement with respect to each other. The tensor $^4\mathbf{C}_*$ characterizes the stiffness of the crystal without regard for the displacement of the sublattices, the tensor $^2\mathbf{C}$ characterizes the stiffness of the crystal with respect to the displacement of the sublattices, and the tensor $^3\mathbf{C}$ describes the mutual influence of two types of deformations. Since we consider the complex lattice, the positive definiteness, according to [8], should take place for the two tensors $^4\mathbf{C}$ and $^2\mathbf{C}$. The fourth-rank tensor $^4\mathbf{C}$ is positively definite in the case when for any nonzero $^2\boldsymbol{\epsilon}$ the following inequality holds true: $^2\boldsymbol{\epsilon}\cdot\cdot{}^4\mathbf{C}\cdot\cdot{}^2\boldsymbol{\epsilon} > 0$. If the condition providing the positive definiteness of the tensor $^2\mathbf{C}$ is not satisfied, there occurs a loss of stability due to the displacement of the sublattices.

The investigation performed in this work demonstrated that, for the majority of the metals marked in Fig. 3, we managed to choose the potential providing the stability properly. However, in a number of cases, we failed to construct the appropriate potential. This is associated with the fact that, for some of the lanthanides and actinides, the distance between the layers is almost two times larger than that for the perfect lattice. For zinc and cadmium, $\zeta \approx 13$–15%, which also proved to be too high.

Table 1 presents the calculated parameters of the potentials for metals in which they provide a stable equilibrium, as well as the magnitudes of the ratios of the left-hand sides of (15) to the maximum dimensionless force which is achieved at the bond breaking.

Table 1. Results of the calculations of the parameters of the potential

Metal	ζ, %	n	m	ρ	ρ_{cut}	$\bar{F}/\bar{f}(b)$	$\bar{F}_e/\bar{f}(b)$
Ce (cerium)	1.33	5.9804	2.1017	0.9259	1.7902	5×10^{-10}	1×10^{-9}
Mg (magnesium)	−0.57	8.7960	2.6601	0.9810	1.6993	2×10^{-9}	2×10^{-8}
Co (cobalt)	−0.60	8.7721	2.5801	0.9806	1.6989	7×10^{-9}	4×10^{-8}
Re (rhenium)	−1.17	8.3911	1.4743	0.9731	1.6901	1×10^{-8}	4×10^{-8}
Tc (technetium)	−1.75	7.1687	1.3537	0.9673	1.6817	9×10^{-9}	3×10^{-8}
Tl (thallium)	−2.12	6.8749	1.2102	0.9647	1.6781	6×10^{-9}	3×10^{-8}
Sc (scandium)	−2.41	6.5200	1.2083	0.9629	1.6749	2×10^{-8}	1×10^{-8}
Zr (zirconium)	−2.48	6.4945	1.2079	0.9628	1.680	3×10^{-9}	2×10^{-8}
Gd (gadolinium)	−2.61	6.3553	1.1832	0.9619	1.6735	4×10^{-9}	3×10^{-8}
Ti (titanium)	−2.76	6.2731	1.1507	0.9612	1.6723	1×10^{-9}	8×10^{-9}
Lu (lutetium)	−2.97	6.1169	1.1413	0.9603	1.6708	6×10^{-11}	3×10^{-9}
Ru (ruthenium)	−3.11	6.0141	1.1379	0.9597	1.6708	4×10^{-9}	3×10^{-9}
Tb (terbium)	−3.18	5.9899	1.1213	0.9595	1.6691	2×10^{-8}	6×10^{-9}
Hf (hafnium)	−3.23	5.9806	1.1053	0.9593	1.6687	1×10^{-8}	3×10^{-9}
Os (osmium)	−3.31	5.9296	1.1007	0.9591	1.6680	4×10^{-9}	3×10^{-8}
Dy (dysprosium)	−3.64	5.8335	1.0400	0.9581	1.6663	1×10^{-8}	2×10^{-8}
Y (yttrium)	−3.79	5.7662	1.0301	0.9578	1.6653	1×10^{-8}	2×10^{-8}
Tm (thulium)	−3.84	5.7586	1.0166	0.9576	1.6650	5×10^{-9}	2×10^{-8}
Er (erbium)	−3.86	5.7585	1.0134	0.9576	1.6650	5×10^{-9}	2×10^{-8}
Ho (holmium)	−3.87	5.7583	1.0101	0.9576	1.6649	5×10^{-9}	3×10^{-8}
Be (beryllium)	−3.98	5.7108	1.0041	0.9573	1.6643	4×10^{-9}	2×10^{-8}

It can be seen from Table 1 that the ratios $\bar{F}/\bar{f}(b)$ and $\bar{F}_e/\bar{f}(b)$ have the order of 10^{-8}–10^{-10}.

A typical graph of interaction forces is presented in Fig. 5. In this figure, the points indicate the forces corresponding to different coordination ellipsoids (the numbers of the ellipsoids are designated by numerals).

The ratios of the elastic constants C_{33}/C_{11} calculated from expressions (10)–(13), (20), and (21) are presented in Table 2 in comparison with the experimental data [26, 27]. The values of the elastic constants measured at the temperature of 4.2 K for all metals, except for Dy (298 K) and Er (81 K), are reported in [26], and the corresponding values obtained at room temperature are given in [27]. The maximum deviation of the theoretical values from the experimental ones is approximately equal to 15%.

5. COMPARISON WITH FACE-CENTERED CUBIC STRUCTURE

The closest packing, which is geometrically represented as a packing of spheres, ensures the minimum internal energy in the crystal. The question now arises as to whether FCC lattice consisting of spheres with appropriate radius is energetically more favorable than the less dense HCP lattice composed of ellipsoids.

Let us consider an FCC lattice in which the atoms interact through the potential defined by expressions (10)–(13). We construct the stress tensor (2) taking into consideration three coordination spheres separated from the reference atom by the distances R^{FCC}, $R^{FCC}\sqrt{2}$, and $R^{FCC}\sqrt{3}$, respectively. In the case of FCC lattice, they are exactly the spheres, because the double distance between the spherical layers is equal to η_0 for all metals. In the first coordination sphere, there are 12 atoms, the second coordination sphere contains 6 atoms, and the third coordination sphere includes 24 atoms. From condition (3), we determine the distance between the nearest neighbor atoms R^{FCC}. A similar procedure is performed for all sets of parameters presented in Table 1. As a result, we find that $R < R^{FCC} < R_0$ for $\zeta < 0$ and $R_0 < R^{FCC} < R$ for $\zeta > 0$. Furthermore, the radius of the fourth coordination sphere $2R^{FCC}$ in all cases proves to be larger than the cut-off radius a_{cut} of the potential.

Next, we have to calculate the energy per atom in HCP and FCC lattices [2, 8]:

$$W = \frac{1}{2N}\sum_{\alpha}\Pi(a_\alpha), \qquad (22)$$

Table 2. Ratio of the elastic constants C_{33}/C_{11}

Metal	Experiment [26]	Experiment [27]	Theory
Ce (cerium)	–	–	1.6561
Mg (magnesium)	1.0468	1.0371	1.1585
Co (cobalt)	1.1693	1.1356	1.1583
Re (rhenium)	1.1077	1.1088	1.1527
Tc (technetium)	–	–	1.1461
Tl (thallium)	1.3559	1.3103	1.1439
Sc (scandium)	–	1.0775	1.1415
Zr (zirconium)	1.1100	1.1528	1.1343
Gd (gadolinium)	1.0677	1.0780	1.1340
Ti (titanium)	1.0818	1.1313	1.1334
Lu (lutetium)	–	–	1.1307
Ru (ruthenium)	1.1290	1.1083	1.1290
Tb (terbium)	–	1.0751	1.1221
Hf (hafnium)	1.0752	1.0884	1.1195
Os (osmium)	–	–	1.1136
Dy (dysprosium)	1.0542	1.0662	1.1172
Y (yttrium)	0.9604	0.9872	1.1117
Tm (thulium)	–	–	1.1106
Er (erbium)	0.9664	1.0071	1.1110
Ho (holmium)	–	1.0405	1.1110
Be (beryllium)	1.1430	1.1952	1.1080

where $N = 38$ (HCP) and $N = 42$ (FCC) are the numbers of atoms that interact with the reference atom; the factor 1/2 is explained by the fact that the potential $\Pi(a_\alpha)$ describes the interaction between two atoms.

The calculations performed in this work demonstrated that, in all cases, the energy per atom in HCP structure is lower than the corresponding energy in FCC structure by approximately 11%. Therefore, the interaction defined by expressions (10)–(13) provides not only the stability of the equilibrium but also the energetic favorability of the geometrically imperfect and, consequently, non-close-packed structure.

6. RESULTS AND CONCLUSIONS

Thus, we have analyzed the possibility of adequately describing HCP structures, which correspond to the packing of the elongated or flattened ellipsoids of revolution in comparison with the sphere along the axis perpendicular to the layer plane (Fig. 2), with the use of the pair force interatomic interaction potential. The potential defined by expressions (10)–(13), which provides the stability of structures with a deviation from the ideal structure of no more than 4%, is obtained from the equilibrium condition. All the parameters of the potential, except for the parameter D, which characterizes the depth of the potential well, are determined by the geometry of the structure and the condition of its equilibrium. The parameter D can be found from a comparison of the results of the calculations with the experimental values of the elastic constants.

It is shown that the potential (10)–(13) correctly describes the structure of the stiffness tensor, because, for example, the ratio of the theoretically obtained elastic constants C_{33}/C_{11} differs from the experimental value by no more than 15% (Table 2).

Furthermore, HCP structure is energetically more favorable than FCC structure in which atoms interact via the same potential (10)–(13). The energy per atom in HCP structure is lower than that in FCC structure by approximately 11%. This effect is similar to that observed when using the pair force interatomic interaction potential in solving the problem of equilibrium of four particles on a plane: either a square or a rhombus with the vertices occupied by the particles can be preferred depending on the width of the potential well [28].

The use of the cut-off radius that does not exceed the double equilibrium distance in the expression for the potential, in combination with a simple formula for the interaction force, can significantly accelerate numerical calculations.

ACKNOWLEDGMENTS

This study was supported by the Russian Foundation for Basic Research (project no. 11-01-00809-a).

REFERENCES

1. A. M. Krivtsov, Phys. Solid State **46** (6), 1055 (2004).
2. A. M. Krivtsov, *Deformation and Fracture of Solids with Microstructure* (Fizmatlit, Moscow, 2007) [in Russian].
3. B. D. Annin, S. N. Korobeinikov, and A. V. Babichev, Sib. Zh. Ind. Mat. **11** (1), 3 (2008).
4. A. Yu. Kuksin, G. E. Norman, V. V. Stegailov, and A. V. Yanilkin, J. Eng. Thermophys. **18** (3), 197 (2009).
5. J. A. Zimmerman, R. E. Jones, and J. A. Templeton, J. Comput. Phys. **229**, 2364 (2010).
6. A. M. Krivtsov and N. F. Morozov, Phys. Solid State **44** (12), 2260 (2002).
7. R. V. Gol'dshtein and A. V. Chentsov, Izv. Akad. Nauk, Mech. Tverd. Tela, No. 4, 57 (2005).
8. A. M. Krivtsov, *Elastic Properties of Monoatomic and Diatomic Crystals* (St. Petersburg State Polytechnical University, St. Petersburg, 2009) [in Russian].
9. I. E. Berinskii, N. G. Dvas, A. M. Krivtsov, et al., *Theoretical Mechanics. Elastic Properties of Monoatomic and Diatomic Crystals*, Ed. by A. M. Krivtsov (St. Petersburg State Polytechnical University, St. Petersburg, 2009) [in Russian].
10. I. E. Berinskiy, A. M. Krivtsov, and A. M. Kudarova, in *Proceedings of the XXXVI Summer School "Advanced Problems in Mechanics," St. Petersburg, Russia, July 6–10, 2008*, p. 122.

11. E. A. Ivanova, A. M. Krivtsov, and N. F. Morozov, Prikl. Mat. Mekh. **71** (4), 595 (2007).
12. D. M. Vasil'ev, *Physical Crystallography* (Metallurgiya, Moscow, 1981) [in Russian].
13. M. S. Daw and M. I. Baskes, Phys. Rev. Lett. **50** (17), 1285 (1983).
14. R. Pasianot and E. J. Savino, Phys. Rev. B: Condens. Matter **45** (22), 12704 (1992).
15. M. I. Baskes and R. A. Johnson, Modell. Simul. Mater. Sci. Eng. **2**, 147 (1994).
16. W. Hu, B. Zhang, B. Huang, F. Gao, and D. J. Bacon J. Phys.: Condens. Matter **13** (6), 1193 (2001).
17. Y.-M. Kim, B.-J. Lee, and M. I. Baskes, Phys. Rev. B: Condens. Matter **74** (1), 014101 (2006).
18. M. A. Baranov, E. A. Dubov, I. V. Dyatlova, and E. V. Chernykh, Phys. Solid State **46** (2), 213 (2004).
19. A. M. Krivtsov and E. A. Podolskaya, Izv. Akad. Nauk, Mekh. Tverd. Tela, No. 3, 77 (2010).
20. V. A. Lagunov and A. B. Sinani, Phys. Solid State **40** (10), 1742 (1998).
21. N. J. Wagner, B. L. Holian, and A. F. Voter, Phys. Rev. A: At., Mol., Opt. Phys. **45** (12), 8457 (1992).
22. WebElements: the Periodic Table on the WWW (http://www.webelements.com/) (Copyright 1993-2010, Mark Winter, The University of Sheffield and WebElements, United Kingdom).
23. *Handbook of Physical Quantities*, Ed. by I. S. Grigoriev and E. Z. Meilikhov (Energoatomizdat, Moscow, 1991; CRC Press, Boca Raton, Florida, United States, 1997).
24. A. I. Lurie, *Nonlinear Theory of Elasticity* (Nauka, Moscow, 1980; North-Holland, Amsterdam, 1990).
25. F. Milstein, Phys. Rev. B: Solid State **4** (3), 1130 (1971).
26. G. Simmons and H. F. Wang, *Single Crystal Elastic Constants and Calculated Aggregate Properties: A Handbook* (Massachusetts Institute of Technology, Cambridge, Massachusetts, United States, 1971).
27. E. A. Brandes and G. B. Brook, *Smithells Metals Reference Book* (Butterworth–Heinemann, Oxford, 1992).
28. N. G. Dvas, in *Proceedings of the XXXIV Summer School "Advanced Problems in Mechanics," St. Petersburg, Russia, June 25–July 1, 2006*, p. 138.